ACS APPLIED MATERIALS & INTERFACES

Research Article

www.acsami.org

Three-Dimensional Conformal Coatings through the Entrapment of Polymer Membrane Precursors

Du T. Nguyen,[‡] Maya Kleiman,[†] Keun Ah Ryu,[†] Stanley Hiew,[†] Kyle Brubaker,[†] Rafik Mughnetsyan,[†] Richard Truong,[†] Benjamin Dolan,[§] Edward Tackett,[§] and Aaron P. Esser-Kahn*[,†]

[†]Department of Chemistry, [‡]Department of Physics and Astronomy, and [§]Rapid Tech, University of California, Irvine, California 92697, United States

Supporting Information

ABSTRACT: We report a technique to coat polymers onto 3D surfaces distinct from traditional spray, spin, or dip coating. In our technique, the surface of a template structure composed of poly(lactic acid) swells and entraps a soluble polymer precursor. Once entrapped, the precursor is cured, resulting in a thin, conformal membrane. The thickness of each coating depends on the coating solution composition, residence time, and template size. Thicknesses ranged from 400 nm to 4 μm within the experimental conditions we explored. The coating method was compatible with a range of polymers. Complicated 3D structures and microstructures of 10 μm thickness and separation were coated using this technique. The templates can also be selectively removed, leaving behind a hollow membrane structure in the shape of the original printed, extruded, or microporous template structures. This technique may be useful in applications that benefit from three-dimensional membrane topologies, including catalysis, separations, and potentially tissue engineering.

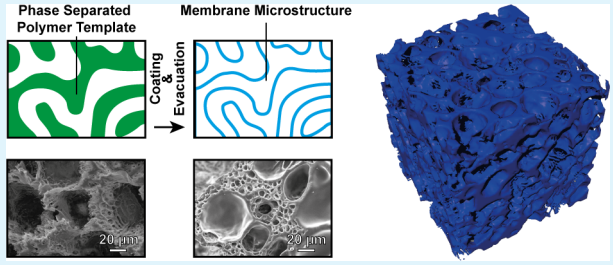

KEYWORDS: *coating, polymer membranes, entrapment, three-dimensional, microstructures*

INTRODUCTION

The ability to coat and deposit materials onto surfaces is one of the most widely used techniques in materials science. Coatings can improve the properties of many materials by changing their surface properties, such as in applications ranging from anticorrosion to semiconducting.[1−5] Processes such as chemical vapor deposition, atomic layer deposition, solution deposition, and layer-by-layer coatings allow for nanoscale depositions.[6−9] Other techniques such as spin coating, dip coating, and electroplating can form thicker coatings.[10−17] For separations applications involving polymeric membranes, a common method is hollow fiber spinning to template the polymeric membrane using solvent dissolution.[18−21] However, few techniques exist that form polymeric membranes with complicated 3D topologies.

Here we report a technique to fabricate microvascular membrane structures through the entrapment of a polymer membrane into a poly(lactic acid) (PLA) template structure. No direct modification of the surface is necessary, making this technique applicable to a wide variety of materials. To coat complicated and fine structures, we sought a technique that did not require thin layer coatings, deposition, or reactivity at the surface. We found that the entrapment of biomolecules and catalysts onto the surfaces of poly(lactic acid) by selectively swelling the surface to incorporate the materials had the potential to develop into a new coating method.[22−24] This procedure was modified to accommodate a variety of polymeric membrane materials. In the templating process, a swollen PLA template surface is used to entrap a membrane precursor from solution. Once entrapped, the precursor is cured to form a membrane conformed to the polymer surface. The polymer template can then be removed, leaving behind the newly formed hollow membrane in the same topology as the original template structure.

For this process, we have characterized the membrane thickness as a function of coating solution composition, structure sizes, and residence times and found that each variable can be used to control membrane thickness ranging from 400 nm to 4 μm. These studies were primarily performed using polydimethylsiloxane (PDMS) as the membrane material, but we also found that many commercial polymers are compatible with the entrapment technique. We demonstrated its application in various 3D structures including 3D printed templates and phase separated microstructures with feature sizes ranging from the millimeter range to the micrometer range. The membranes are strong enough to retain liquids and have porosities suitable for the selective separation of gases.

To perform an entrapment, an appropriate coating solution must be comprised of four elements: template (PLA), template solvent, template nonsolvent, and membrane precursor (Figure 1). A prefabricated microstructure is placed into the coating solution, which swells the PLA template without fully dissolving

Received: November 27, 2013
Accepted: January 17, 2014
Published: January 17, 2014

   dx.doi.org/10.1021/am4053943 | ACS Appl. Mater. Interfaces 2014, 6, 2830−2835

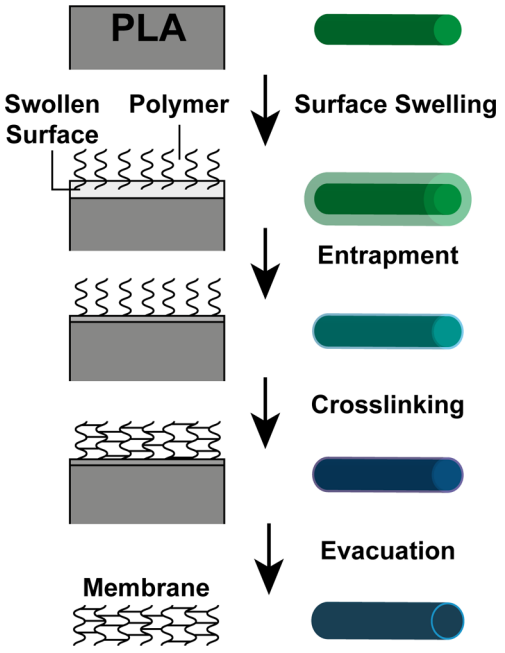

Figure 1. Entrapment process schematic. In the first step of the entrapment process, a polymer template is swollen in a solvent/nonsolvent mixture containing the membrane precursor. Next, the polymer template is deswelled, entrapping the membrane precursor. The precursor is then cured to form the membrane at the surface of the template. Last, the template can be removed, leaving behind a hollow membrane conformed to the topology of the template.

it, and results in a thin area in which the template is swollen. The membrane precursor enters this swollen region and becomes entrapped when the surface deswells. The structure is then deswelled by either rinsing in a nonsolvent, or by centrifugation to remove the coating solution. Once the template has deswollen, the membrane precursor can be cured, forming a 3D conformal coating of the template polymer structure. In this technique, several parameters affect the resulting membrane including the solution composition, template residence time, and the characteristic size scale of the template. PLA was chosen as the template, as it can be selectively removed through solvent dissolution or the vaporization of a sacrificial component (VaSC), leaving behind a membrane shaped from the initial template.[25−27]

EXPERIMENTAL SECTION

Materials. Polydimethylsiloxane (PDMS) was obtained from Dow Corning. Dioxane, hexane, acetone, isopropanol, N-Methyl-2-pyrrolidone (NMP), Dichloromethane (DCM), chloroform, monoethanolamine, polycaprolactone (average M_n 45 000), and poly(vinyl alcohol) (average M_w 85 000−146 000) were obtained from Sigma Aldrich. Dow Corning 736 Sealant, epoxy, urethane, and acrylic adhesives were purchased from McMasterCarr (part numbers 74515A32, 7541A83, 7448A22, and 75395A65, respectively). RTV 430 was obtained from Momentive. Poly(lactic acid) was supplied by Teijin Monofilament. Matrimid was supplied by Hunaid Nulwala, Carnegie Mellon University.

General Entrapment Coating Procedure (for PDMS). PDMS precursor is made by mixing the PDMS base composed of alkene terminated siloxanes with the curing agent, a standard platinum hydrosilation chemistry, in a 10:1 ratio. The precursor is degassed under vacuum for 10 min. Next, a 10 mL ternary solution consisting of the precursor, dioxane (solvent), and hexane (nonsolvent) is mixed at the desired concentrations. A 2 cm length of PLA fiber with the desired diameter, ranging from 100 to 500 μm, is placed into the coating solution. After times ranging from 1 min to 2 h, the fiber is removed and rinsed in hexane for 5 s. Last, the coated fiber is then heated to 85 °C for 30 min to cure the PDMS membrane.

Thickness Characterization. We characterized the thicknesses of the newly formed membranes with respect to the solution composition, residence time, and template size scale. The characterizations were conducted using PDMS as the membrane material and 300 μm PLA microfibers, pretreated for the VaSC microfabrication technique, as the template structures.[27] The VaSC technique allows for the depolymerization of the PLA template, converting the solid template into gas under heat and vacuum. The general entrapment coating procedure was modified to accommodate a range of times, sizes, and compositions. The coated fibers were placed in a secondary support casing of PDMS and removed via VaSC at 200 °C, resulting in a hollow microchannel within PDMS. Cross sections of the microchannel were imaged using scanning electron microscopy (SEM). We distinguished the conformal membrane as it had different grain characteristics than the secondary support when imaged under SEM. We examined the cross sections for quantitative measurements of the membrane thicknesses at several locations along the fiber circumference. Data was represented as the average ± standard deviation (n = 10). Using FTIR spectroscopy, the free-standing membranes fabricated through the entrapment method were confirmed to be PDMS, and not a mixture of PDMS and PLA (see the Supporting Information).

Coatings on 3D Printed Structures. The 3D printed PLA templates were printed by RapidTech, a UCI user institution, using an Airwolf AW3D V5.5 3D printer. Designs for the 3D templates were obtained from Thingiverse (thingiverse.com). An initial PDMS membrane was coated onto the templates using a 12.5:75:12.5 (PDMS:Hexane:Dioxane) solution composition. The coating was performed with a residence time of 1 h in the coating solution at an elevated temperature of 65 °C. This would partially cure the entrapped precursor, allowing for a thicker membrane and clearer visualization. The membrane was then fully cured at 85 °C for 30 min. For some experiments, an additional coating was added to increase the thickness of the membrane. For these experiments, two additional coatings of PDMS were performed using a similar coating method. However, the solution composition was 9:36:55 (PDMS:Hexane:Isopropanol) in order to swell the initial PDMS membrane rather than the PLA template. Once the PLA templates were coated with the additional membranes, sections of the membranes were removed to allow the PLA to exit the membrane. The PLA templates were removed using solvent dissolution in dioxane for over 24 h. Solvent dissolution was used rather than VaSC since the solvent would readily enter the resulting membrane and aid its three-dimensional suspension for clear visualization. The resulting hollow membranes were transferred to acetone for enhanced visual clarity because of the larger difference in index of refraction between PDMS and acetone.

3D Microstructure Coatings. Microstructured PLA templates were fabricated through the temperature induced phase separation of PLA.[28,29] In temperature induced phase separation, a homogeneous mixture of a polymer and solvent is made at an elevated temperature. Upon letting the homogeneous mixture cool, the mixture becomes thermodynamically unstable and separates into a polymer lean phase and a polymer-rich phase. Under the proper conditions, these phases can separate into a bicontinuous structure. Briefly, 9 wt % PLA was dissolved in a dioxane/water mixture (87:13 dioxane:water) at 85 °C. The solution was then phase separated by lowering the temperature to 15 °C for 1 h. Last, the solution was frozen by immersing it into liquid nitrogen and the resulting frozen material was lyophilized for 8 h to remove the dioxane and water, leaving a microporous bicontinuous PLA. Following the fabrication of the template, multiple coatings were deposited onto the template following the procedure given for 3D-printed structure coatings. The coating solutions were removed using centrifugation as the dense porous structure of the template made solvent exchange very slow. The templates were then removed using the VaSC process.

Characterization. Characterization of membrane topologies were performed using SEM and X-ray computed tomography (μCT). SEM images were acquired using a Philips XL-30 FEG SEM. Three dimensional μCT images were acquired using an Xradia VersaXRM 410 CT system under 20X magnification. FTIR spectroscopy was conducted using a PerkinElmer System 2000 FTIR. Image processing was performed using the ImageJ image processing and analysis software. 3D reconstruction of the μCT slices were performed using the BoneJ plugin for ImageJ.

DISCUSSION

Our primary interest was in controlling membrane thickness, so we examined the composition of the ternary solvent–nonsolvent–membrane precursor mixture and its effect on membrane thickness (Figure 2). PDMS membranes were coated onto 300 μm diameter PLA fibers using ternary compositions (with ranges from 10 to 60% PDMS, 30–80% hexane, and 10–60% dioxane, by volume) with a residence time of 1 h. Hexane was chosen as the solvent for PDMS, whereas dioxane was the solvent for PLA. Other combinations of solvents might also be used.

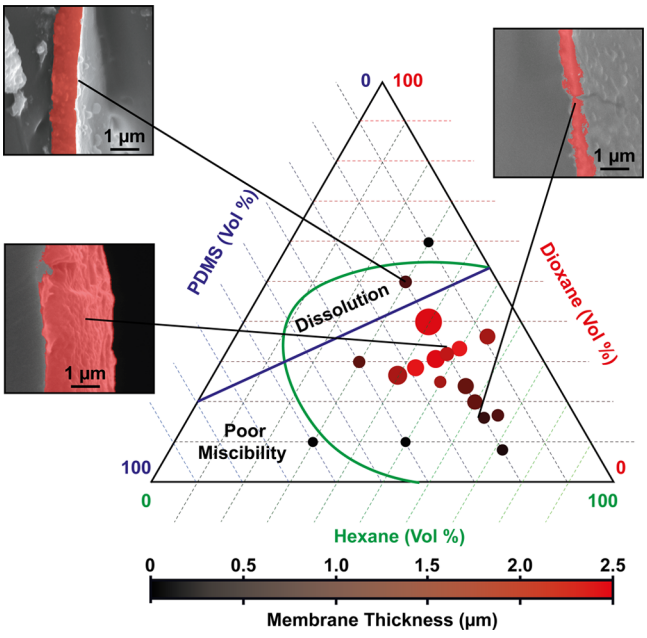

Figure 2. Effect of coating solution composition. The three parts of the coating solution are represented in a ternary plot of the solvent (dioxane), nonsolvent (hexane), and membrane precursor concentrations (PDMS). Data are presented as average ± standard deviation (n = 10). The size of the data points indicates the uncertainty in the thickness measurements, with larger circles having larger uncertainties (see the Supporting Information). Above a threshold solvent concentration, the polymer template can dissolve, resulting in no membrane formation. When the composition is too high in the nonsolvent (if the precursor is not miscible in the nonsolvent), a region of poor miscibility exists which prevents the entrapment of the precursor. Conditions of good miscibility and large swelling (but not dissolution) are necessary to achieve the thickest membranes. For clarity, membranes are false colored red in SEM images.

We found that in order to form a coating, all components of the ternary mixture must be miscible and that the template solvent must not dissolve the template within the coating time scale. The mixture can step out of this coating region when the mixture contains a low concentration of hexane, high concentration of PDMS, or high concentration of dioxane. As a general trend, the thickest membranes occur close to the boundary between the coating region and the dissolution region. However, the thickness decreases once the mixture enters the dissolution region. Our operating hypothesis is that a smaller entrapping layer is being formed. With too high a dissolving solvent percentage, the outer edge of the entrapping layer may completely dissolve, resulting in a smaller entrapping layer once the fiber deswells. (Figure 2)

Next, we examined the effects of the characteristic size of the template structure by coating fibers of different diameters, ranging from 100 to 500 μm. The coating residence time was 1 h and the solution composition was 33:40:27 (PDMS:hexane:dioxane, volumetric ratio), a pairing we determined from previous experiments would create membranes of 1.7 ± 0.4 μm thickness in a 300 μm fiber. As the characteristic size increases, the thickness of the membrane also increases (Figure 3) ranging from 0.7 to 3.8 μm. Though not seen in these experiments, there is likely an upper limit to the change in membrane thickness with respect to the characteristic size. The maximum thickness corresponds roughly to the maximum swollen state of the template.

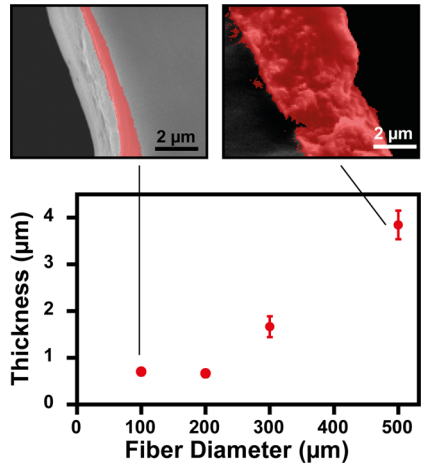

Figure 3. Template size scale. Several diameter PLA fibers were coated with the PDMS membrane. The thickness of the resulting membrane was measured. As the fiber diameter increased, so did the membrane thickness. Data is presented as average ± standard deviation (n = 10). For clarity, membranes are false colored red in SEM images.

Last, we examined the effects of residence time spent in the entrapment solution. The coatings were performed on 300 μm diameter microchannels using a solution composition of 16:68:16 (PDMS: Hexane: Dioxane, volumetric ratio). This composition was chosen for its lower dioxane concentration so that the fiber would not dissolve during the range of residence times. Here, we observed that as the residence time increases, so does the membrane thickness (Figure 4). The membrane thicknesses were between 0.5 to 1.4 μm for residence times ranging from 1 to 120 min. Unfortunately, longer residence times resulted in less uniform membranes (uncertainties increasing from ±0.1 μm to ±0.4 μm). Our current hypothesis is that the increased residence time creates a larger intermediate region of swollen PLA. When the region deswells, the volume of entrapped polymer must return to the same initial volume. This larger change likely results in a decrease in uniformity.

After characterizing this technique with respect to the solution composition, characteristic size scale, and residence time, we tested the scope of polymers amenable to our solution

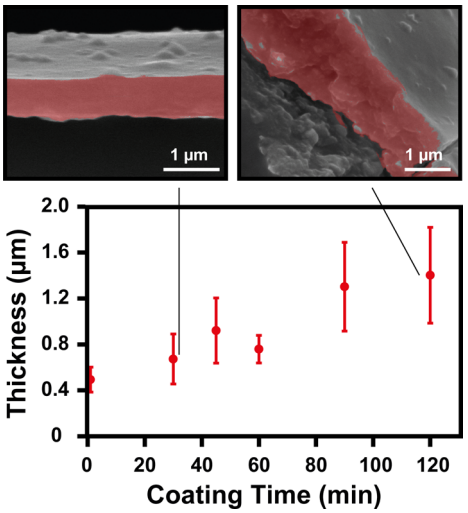

Figure 4. Residence time in coating solution. Increased residence times resulted in increased membrane thicknesses. At residence times as low as 5 s, a thin membrane (<1 μm) forms. As the residence times increased, the uniformity of the coatings also decreased. Data are presented as average ± standard deviation (n = 10). For clarity, membranes are false colored red in SEM images.

coating technique. These polymers included other silicon-based rubbers, two-part adhesive epoxy mixtures, and conventional condensation polymers (Table 1). However, all of these

Table 1. Other Entrapment Membranes[a]

membrane base	template solvent	template nonsolvent
PDMS	dioxane	water
PDMS/PIM[37]	dioxane	hexane
poly(vinyl) alcohol	dioxane	water
polycaprolactone	chloroform	water
nylon	dioxane	hexane/water
matrimid	DCM	NMP
acrylic	acetone	hexane
epoxy	DCM	isopropanol
polyurethane	DCM	hexane
Dow Corning 736 sealant	dioxane	hexane
silicon RTV 430	dioxane	hexane

[a]A general screen of other possible membrane materials was conducted in order to determine if the entrapment method of membrane coating was a general technique. Some mixtures displayed poor miscibility, but still formed a coating.

employed the same general method of entrapping the membrane material in the template using a solvent−nonsolvent-membrane precursor solution. The membranes were coated onto 300 μm PLA fibers using a solution composition of 12.5:75:12.5 (membrane precursor:solvent:nonsolvent, volumetric ratio). Because of the different membrane materials, some had smaller miscibility regions. This composition was chosen to keep all membrane materials within the miscibility region. As we wanted only to verify membrane formation, the fibers were removed using solvent dissolution of the fibers. The presence of a hollow tube confirmed the membrane formation (see the Supporting Information). The many different fabricated polymer membranes confirmed that this technique is compatible with a wide range of substrates, beyond the initial characterization of PDMS membranes. These polymeric membranes might find potential uses in high-surface-area supports for separations, catalysis, and desalinization.

We then demonstrated the versatility of the coating method for various template geometries by coating a range of complicated 3D structures. One complicated structure formed was a helical microchannel pair (see the Supporting Information). Two template PLA fibers are coated to form an initial membrane and then twisted together to form a helix. The fibers are surrounded by a support of bulk PDMS and removed using VaSC. The two resulting microchannels remain in close contact, but are separated by the initial membrane formed by the coatings with an estimated separation of 5 μm. Two different color dyes were flowed through each microchannel to confirm that there was no microscale leaking between the two microchannels. Positioning separated microchannels at submicrometer distances can have potentially useful applications in microvascular designs.

We also used the helical structure to check for the presence of defects in the membrane by measuring its gas permeability. If defects were present, they would result in higher gas permeability than predicted for the membrane material. The permeability of the membrane was determined by measuring the mass transfer rate of CO_2 from one channel to the other in the pair using a colorimetric detection method.[25,26] The membrane was calculated to have a permeability of 4300 Barrer, which is within the range of reported PDMS permeabilities.[20,21] We also examined a microvascular system with known defects caused by the overetching of the PDMS membrane.[26,30] When defects are present, the permeability was calculated to be 6100 Barrer (see the Supporting Information).

We then determined if our technique was compatible with 3D printing by fabricating sets of hollow membrane structures using 3D printing of PLA (Figure 5). Following the entrapment of PDMS onto the 3D printed structures, the PLA was dissolved, leaving behind a hollow shell of the structure. These structures represented the largest size scale of the membrane coating process (5 mm). Multiple coatings of PDMS were also applied to these structures to aid in visual clarity and resulted in membrane thicknesses of 10 μm. The multiple coatings were obtained using a ternary coating solution designed to swell the initial PDMS coated layer rather than the PLA surface (PDMS, Hexane, and Isopropanol). This approach provides a unique pathway to fabricate hollow microstructures that would otherwise be difficult to 3D print, with potential uses in fields such as tissue engineering.

The last demonstration of the entrapment technique allowed for the coating of high specific surface area PLA formed through thermally induced phase separation (Figure 6).[28,29] In thermally induced phase separation, a polymer/solvent/nonsolvent solution can phase separate to create a highly interconnected polymer network. Under optimal conditions, this network can be completely bicontinuous (spinodally phase separated), allowing for the formation of a conformal membrane structure. When followed by lyophilization and the removal of the solvent/nonsolvent mixture, the polymer retains this form and obtains a high specific surface area. These structures were coated with PDMS and evacuated to leave behind a hollow membrane microstructure. SEM imaging confirmed the presence of a conformal membrane microstructure. This allows for the creation of a free-standing, membrane structure with an estimated specific surface area of 57 000 m^2/m^3. The specific surface area was calculated using 3D reconstruction of the μCT slices. The image processing

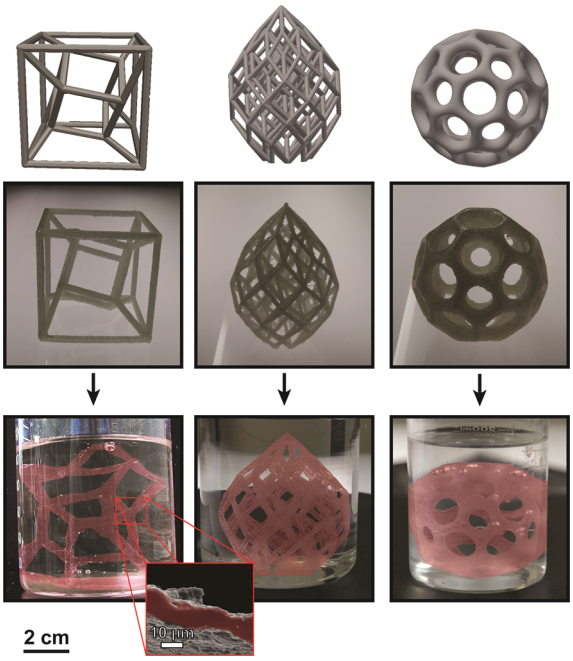

Figure 5. 3D printed template coatings. Using a 3D printer, several three-dimensional PLA structures were formed. Multiple coatings of PDMS were placed around these structures and the templates were evacuated leaving behind hollow membrane structures. The membranes were left in acetone and false colored red to maintain and highlight the membrane structure.

software automatically calculates the surface area of the 3D object although the volume is the μCT scan volume. Surface areas were set as the interface between the membrane and air. However, the presence of defects in this membrane has not been verified.

CONCLUSION

In conclusion, we have adapted a method for the coating of polymer template structures and shown its compatibility with a range of polymeric materials and geometries. This coating method was used in conjunction with our template removal process, VaSC, and resulted in hollow membrane structures that were replicas of the initial templates. Several parameters can affect the thicknesses of the membranes formed, including the coating solution composition, residence time, and template size scale. The method is general enough to form coatings of a wide variety of membrane structures. The method was shown to work on a variety of size scales from 100 μm to 5 mm and could conform onto a number of three-dimensional structure, as demonstrated by the coating of 3D printed objects and thermally induced phase separated templates. Our new polymer membrane coating technique enables coating of many new materials and geometries, which should lead to new applications and designs in microvascular structures, self-healing composites, and membrane separations.[31−36]

ASSOCIATED CONTENT

Supporting Information

PDMS membrane and PLA film FTIR data (Figure S1). Images of other entrapment membranes (Figure S2). Membrane permeability calculations and measurements (Figure S3). Entrapment solution composition thickness summary (Table S1). This material is available free of charge via the Internet at http://pubs.acs.org.

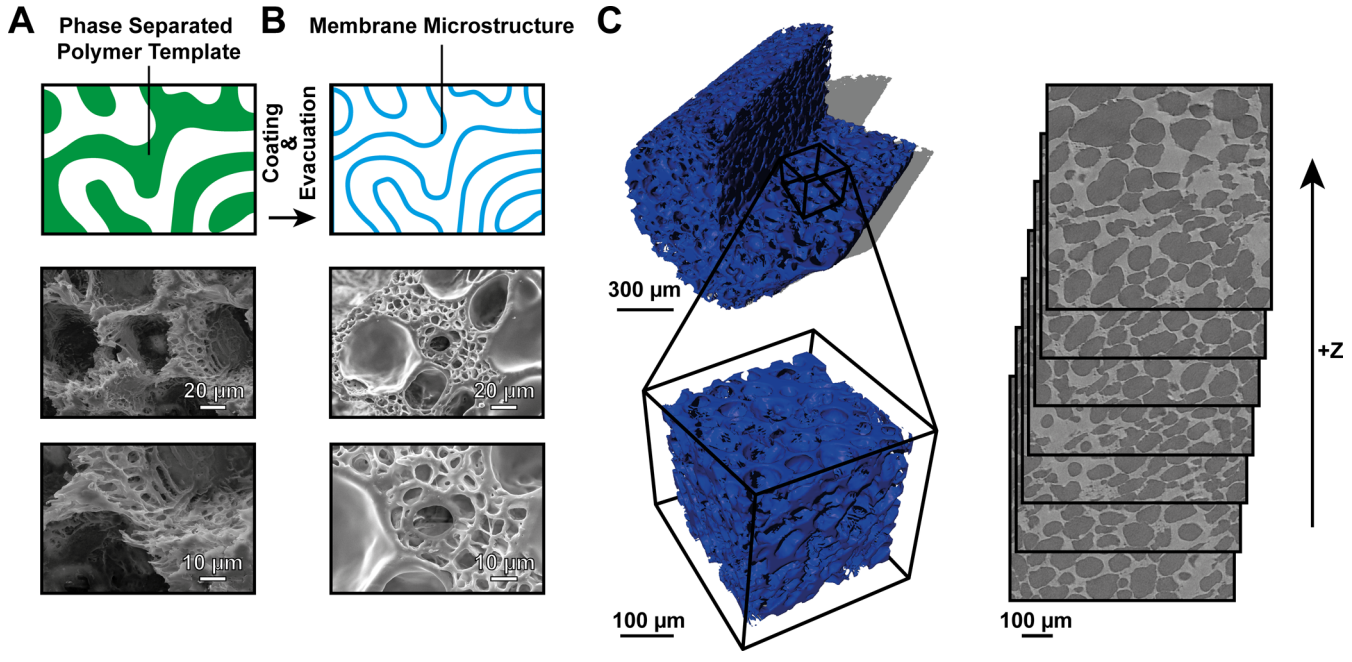

Figure 6. Thermally induced phase-separated template coatings. (A) Three-dimensional microstructures were formed by thermally inducing phase separation of PLA, resulting in a highly interconnected and three-dimensional polymer microstructure. (B) Evacuated membrane structure. The thermally phase-separated structures were coated with PDMS and the templates were removed through the VaSC technique. (C) μCT membrane structure. A three-dimensional view of the template membrane structure is shown. The specific surface area of the structure was calculated using the BoneJ plugin for ImageJ during 3D reconstruction. A rotational μCT image can be found in the Supporting Information.

AUTHOR INFORMATION

Corresponding Author

*E-mail: aesserka@uci.edu.

Notes

The authors declare no competing financial interest.

ACKNOWLEDGMENTS

This work was supported by the AFOSR Young Investigator Program under FA9550-12-1-0352, an ACS-PRF award under 53493-DN110, and a 3M Non-Tenured Faculty Award. D.T.N. was supported by the Department of Defense (DoD) through the National Defense Science & Engineering Graduate Fellowship (NDSEG) Program. The authors acknowledge Dean of HSSoE at UCI for support of Rapid Tech and James Neal for helpful discussion.

REFERENCES

(1) Talo, A.; Passiniemi, P.; Forsén, O.; Yläsaari, S. Polyaniline/epoxy Coatings with Good Anti-Corrosion Properties. *Synth. Met.* **1997**, *85*, 1333−1334.

(2) Hamdy, A. S. Advanced Nano-Particles Anti-Corrosion Ceria Based Sol Gel Coatings for Aluminum Alloys. *Mater. Lett.* **2006**, *60*, 2633−2637.

(3) Krebs, F. C. Fabrication and Processing of Polymer Solar Cells: A Review of Printing and Coating Techniques. *Sol. Energy Mater. Sol. Cells* **2009**, *93*, 394−412.

(4) Hu, L.; Kim, H. S.; Lee, J.-Y.; Peumans, P.; Cui, Y. Scalable Coating and Properties of Transparent, Flexible, Silver Nanowire Electrodes. *ACS Nano* **2010**, *4*, 2955−2963.

(5) Oh, S. W.; Myung, S.-T.; Oh, S.-M.; Oh, K. H.; Amine, K.; Scrosati, B.; Sun, Y.-K. Double Carbon Coating of $LiFePO_4$ as High Rate Electrode for Rechargeable Lithium Batteries. *Adv. Mater.* **2010**, *22*, 4842−4845.

(6) Ozaydin-Ince, G.; Coclite, A. M.; Gleason, K. K. CVD of Polymeric Thin Films: Applications in Sensors, Biotechnology, Microelectronics/organic Electronics, Microfluidics, MEMS, Composites and Membranes. *Rep. Prog. Phys.* **2012**, *75*, 016501.

(7) Ritala, M.; Niinistö, J. In *Chemical Vapor Deposition*; Jones, A. C.; Hitchman, M. L., Eds.; Royal Society of Chemistry: Cambridge, U.K., 2009; Chapter 4, pp 158−206.

(8) Chen, W.; McCarthy, T. J. Layer-by-Layer Deposition: A Tool for Polymer Surface Modification. *Macromolecules* **1997**, *30*, 78−86.

(9) Knez, M.; Nielsch, K.; Niinistö, L. Synthesis and Surface Engineering of Complex Nanostructures by Atomic Layer Deposition. *Adv. Mater.* **2007**, *19*, 3425−3438.

(10) Brinker, C. J.; Frye, G. C.; Hurd, A. J.; Ashley, C. S. Fundamentals of Sol−Gel Dip Coating. *Thin Solid Films* **1991**, *201*, 97−108.

(11) Lively, R. P.; Mysona, J. A.; Chance, R. R.; Koros, W. J. Formation of Defect-Free Latex Films on Porous Fiber Supports. *ACS Appl. Mater. Interfaces* **2011**, *3*, 3568−3582.

(12) Stillwagon, L. E.; Larson, R. G. Leveling of Thin Films over Uneven Substrates during Spin Coating. *Phys. Fluids Fluid Dyn.* **1990**, *2*, 1937.

(13) Scriven, L. E. Physics and Applications of DIP Coating and Spin Coating. *MRS Proc.* **2011**, *121*.

(14) Yanagishita, H.; Kitamoto, D.; Haraya, K.; Nakane, T.; Okada, T.; Matsuda, H.; Idemoto, Y.; Koura, N. Separation Performance of Polyimide Composite Membrane Prepared by Dip Coating Process. *J. Membr. Sci.* **2001**, *188*, 165−172.

(15) Hall, D. B.; Underhill, P.; Torkelson, J. M. Spin Coating of Thin and Ultrathin Polymer Films. *Polym. Eng. Sci.* **1998**, *38*, 2039−2045.

(16) Lawrence, C. J. The Mechanics of Spin Coating of Polymer Films. *Phys. Fluids* **1988**, *31*, 2786.

(17) Frazier, A. B.; Allen, M. G. Metallic Microstructures Fabricated Using Photosensitive Polyimide Electroplating Molds. *J. Microelectromech. Syst.* **1993**, *2*, 87−94.

(18) Lively, R. P.; Chance, R. R.; Kelley, B. T.; Deckman, H. W.; Drese, J. H.; Jones, C. W.; Koros, W. J. Hollow Fiber Adsorbents for CO_2 Removal from Flue Gas. *Ind. Eng. Chem. Res.* **2009**, *48*, 7314−7324.

(19) Clausi, D. T.; Koros, W. J. Formation of Defect-Free Polyimide Hollow Fiber Membranes for Gas Separations. *J. Membr. Sci.* **2000**, *167*, 79−89.

(20) Corti, A. Carbon Dioxide Removal in Power Generation Using Membrane Technology. *Energy* **2004**, *29*, 2025−2043.

(21) Powell, C. E.; Qiao, G. G. Polymeric CO_2/N_2 Gas Separation Membranes for the Capture of Carbon Dioxide from Power Plant Flue Gases. *J. Membr. Sci.* **2006**, *279*, 1−49.

(22) Dong, H.; Esser-Kahn, A. P.; Thakre, P. R.; Patrick, J. F.; Sottos, N. R.; White, S. R.; Moore, J. S. Chemical Treatment of Poly(lactic Acid) Fibers to Enhance the Rate of Thermal Depolymerization. *ACS Appl. Mater. Interfaces* **2012**, *4*, 503−509.

(23) Rasal, R. M.; Janorkar, A. V.; Hirt, D. E. Poly(lactic Acid) Modifications. *Prog. Polym. Sci.* **2010**, *35*, 338−356.

(24) Quirk, R. A.; Davies, M. C.; Tendler, S. J. B.; Shakesheff, K. M. Surface Engineering of Poly(lactic Acid) by Entrapment of Modifying Species. *Macromolecules* **2000**, *33*, 258−260.

(25) Nguyen, D. T.; Leho, Y. T.; Esser-Kahn, A. P. A Three-Dimensional Microvascular Gas Exchange Unit for Carbon Dioxide Capture. *Lab Chip* **2012**, *12*, 1246−1250.

(26) Nguyen, D. T.; Leho, Y. T.; Esser-Kahn, A. P. The Effect of Membrane Thickness on a Microvascular Gas Exchange Unit. *Adv. Funct. Mater.* **2013**, *23*, 100−106.

(27) Esser-Kahn, A. P.; Thakre, P. R.; Dong, H.; Patrick, J. F.; Vlasko-Vlasov, V. K.; Sottos, N. R.; Moore, J. S.; White, S. R. Three-Dimensional Microvascular Fiber-Reinforced Composites. *Adv. Mater.* **2011**, *23*, 3654−3658.

(28) Tanaka, T.; Lloyd, D. Formation of Poly(l-Lactic Acid) Microfiltration Membranes via Thermally Induced Phase Separation. *J. Membr. Sci.* **2004**, *238*, 65−73.

(29) Nam, Y. S.; Park, T. G. Biodegradable Polymeric Microcellular Foams by Modified Thermally Induced Phase Separation Method. *Biomaterials* **1999**, *20*, 1783−1790.

(30) Takayama, S.; Ostuni, E.; Qian, X.; McDonald, J. C.; Jiang, X.; LeDuc, P.; Wu, M.-H.; Ingber, D. E.; Whitesides, G. M. Topographical Micropatterning of Poly(dimethylsiloxane) Using Laminar Flows of Liquids in Capillaries. *Adv. Mater.* **2001**, *13*, 570−574.

(31) Bellan, L. M.; Kniazeva, T.; Kim, E. S.; Epshteyn, A. A.; Cropek, D. M.; Langer, R.; Borenstein, J. T. Fabrication of a Hybrid Microfluidic System Incorporating Both Lithographically Patterned Microchannels and a 3D Fiber-Formed Microfluidic Network. *Adv. Healthcare Mater.* **2012**, *1*, 164−167.

(32) Zheng, Y.; Henderson, P. W.; Choi, N. W.; Bonassar, L. J.; Spector, J. A.; Stroock, A. D. Microstructured Templates for Directed Growth and Vascularization of Soft Tissue in Vivo. *Biomaterials* **2011**, *32*, 5391−5401.

(33) Zhang, A.; Chen, M.; Du, C.; Guo, H.; Bai, H.; Li, L. Poly(dimethylsiloxane) Oil Absorbent with a Three-Dimensionally Interconnected Porous Structure and Swellable Skeleton. *ACS Appl. Mater. Interfaces* **2013**, *5*, 10201−10206.

(34) Toohey, K. S.; Hansen, C. J.; Lewis, J. A.; White, S. R.; Sottos, N. R. Delivery of Two-Part Self-Healing Chemistry via Microvascular Networks. *Adv. Funct. Mater.* **2009**, *19*, 1399−1405.

(35) Bettinger, C. J.; Weinberg, E. J.; Kulig, K. M.; Vacanti, J. P.; Wang, Y.; Borenstein, J. T.; Langer, R. Three-Dimensional Microfluidic Tissue-Engineering Scaffolds Using a Flexible Biodegradable Polymer. *Adv. Mater.* **2006**, *18*, 165−169.

(36) Balasubramanian, A.; Morhard, R.; Bettinger, C. J. Shape-Memory Microfluidics. *Adv. Funct. Mater.* **2013**, *23*, 4832−4839.

(37) Budd, P. M.; Elabas, E. S.; Ghanem, B. S.; Makhseed, S.; McKeown, N. B.; Msayib, K. J.; Tattershall, C. E.; Wang, D. Solution-Processed, Organophilic Membrane Derived from a Polymer of Intrinsic Microporosity. *Adv. Mater.* **2004**, *16*, 456−459.